Detection and Estimation of Multiplexed Soliton Signals

Andrew C. Singer, *Member, IEEE* Alan V. Oppenheim, *Fellow, IEEE,* and Gregory W. Wornell, *Member, IEEE*

***Abstract*—Solitons are eigenfunction solutions to certain nonlinear wave equations that arise in a variety of natural and man-made systems. Their rich properties and tractability make them an intriguing component of such systems, often describing large-scale or long-term behavior of natural systems, or the information content in certain communication or signal processing systems. However, it is often difficult to detect or estimate the parameters of solitons in such systems due to the presence of strong nonsoliton components or the nonlinear interaction of multiple solitons. The objective of this paper is to develop and investigate the detection and estimation of soliton signals. As a framework for this study, we consider using these nonlinear systems as both signal generators and signal processors in a form of multiplexed soliton communication. In contrast to more conventional uses of solitons in a communications context, our communication system uses soliton systems for signal generation and multiplexing for transmission over traditional linear channels. In addition to their mathematical tractability and the simplicity of the analog circuits used to generate and process them, we show that the soliton signal dynamics may also provide a mechanism for decreasing transmitted signal energy while enhancing signal detection and parameter estimation performance.**

***Index Terms*—Estimation, modulation, multiplexing, nonlinear circuits, signal detection, solitons.**

I. Introduction

SOLITONS are stable, mode-like solutions to a special class of nonlinear wave equations that can be solved analytically using a technique known as "inverse scattering" [1]. The inverse scattering transform can be interpreted as a nonlinear Fourier analysis for these systems, which decompose wave dynamics into a superposition of normal modes. These normal modes are solitons, and their particle-like properties have been observed in a variety of natural phenomena including ocean and plasma waves [2], [3], crystal lattice vibrations [4], and energy transport in proteins [2]. Solitons also describe the behavior of a variety of man-made systems, including superconducting transmission lines [5], nonlinear circuits [6], [7], ultrafast electronics and optoelectronics [8], [9], and surface acoustic wave devices [10].

Manuscript received April 17, 1997; revised January 18, 1999. The associate editor coordinating the review of this paper and approving it for publication was Dr. Ali H. Sayed.

A. C. Singer is with the Department of Electrical and Computer Engineering, University of Illinois at Urbana-Champaign, Urbana, IL 61801 USA.

A. V. Oppenheim and G. W. Wornell are with the Department of Electrical Engineering, Massachusetts Institute of Technology, Cambridge, MA 02139 USA.

Publisher Item Identifier S 1053-587X(99)07650-3.

From an engineering standpoint, these nonlinear wave equations provide useful models for analyzing natural phenomena as well as the behavior of certain electrical and physical systems. They also constitute building blocks for more complex, yet analytically tractable, signal processing or communication systems. However, in many contexts, it is often difficult to observe solitons in physical systems with rich dynamics since solitons can be masked by strong nonsoliton modes. For example, solitons present as internal waves or as surface waves in many ocean environments can be obscured by energetic radiation modes [11]. In addition, when multiple interacting solitons are present, it can be difficult to resolve or measure them, as is the case for densely wavelength-multiplexed optical solitons in fiber [12]. For a number of applications, it is important to develop effective techniques for detecting and estimating the parameters of solitons from noisy measurements.

Recently, circuit implementations of certain nonlinear systems that can generate and process analog signals containing solitons, or "soliton signals," were developed in [13] and were presented in [14]. The focus of that paper is on the implementation of a class of soliton systems with analog circuitry and a statistical characterization of their operation in the presence of additive disturbances. In this paper, parameter estimation and detection of soliton signals are considered for this class of systems.

As a framework for exploring detection and estimation of soliton signals, we consider using these nonlinear systems as both signal generators and signal processors in a new multiplexed communication system over traditional linear channels such as coaxial cable or radio frequency broadcast. In the process, we suggest a speculative but plausible communication paradigm in which the parameters of soliton signals are modulated and the nonlinear interaction among solitons is exploited to multiplex signal streams. Parameter estimation and detection for these soliton signals then directly address many of the performance aspects of the proposed communication system.

A plausible scenario in which such a soliton multiplexing system might be used is one where multiple signals or data streams are present at a transmitter that can efficiently combine and transmit them over a wideband linear channel. Multiplexing strategies that combine data and jointly encode or modulate them are capable of exploiting the additional coordination for enhanced receiver performance. While joint encoding (and

1053–587X/99$10.00 © 1999 IEEE

decoding) of multiple streams in general has a complexity that increases with the number of streams, the soliton modulation and multiplexing techniques developed in this paper have a fixed receiver structure.

One potential benefit to using solitons as carrier signals and the nonlinear systems as multiplexors is that, as we will show, the soliton signal dynamics provide a mechanism for simultaneously decreasing transmitted signal energy and enhancing communication performance. More broadly, there has been a resurgence of interest in analog modulation and coding techniques [15] in efforts to develop communication systems for a variety of broadcast and multicasting scenarios where digital techniques are suboptimal. In this context, this soliton communication system can, in principle, be viewed as a simple form of joint modulation and analog error protection with convenient hardware implementations.

In order to develop this framework, some of the well-known properties of solitons are briefly described in Section II. The remainder of the paper focuses on new ideas and results. In Section III, a communication paradigm is introduced where soliton signals are used as carrier waveforms whose parameters are modulated with information-bearing signals. The associated nonlinear systems can multiplex multiple signals and independently extract them by exploiting the eigenfunction properties of solitons for these systems. The methods and analysis in this paper center mainly on the Toda lattice: a particular nonlinear system that supports soliton solutions and whose implementation via analog circuitry is discussed in detail in [14]. This system, which is described in Section II along with some of the properties of its soliton solutions, forms the basis of a soliton communication paradigm developed in Section IV. In Section V, the effects of unknown channel gain and signal corruption on the dynamics of solitons in the Toda lattice and the processed noise statistics are analyzed, extending the statistical characterization developed in [14] with an analysis based on the inverse scattering transform.

The extent to which the parameters of these soliton signals can be reliably estimated in noise has a significant impact on potential communication applications. Accordingly, Cramér–Rao bounds on parameter estimation error are examined in Section VI. Based on a statistical characterization of the received and processed soliton signals, a set of parameter estimation algorithms are presented in which maximum-likelihood (ML) estimates can be obtained from corrupted measurements. In Section VII, we demonstrate how soliton circuits can be used to enhance the detection of multiplexed solitons in noise. Section VIII contains some concluding remarks.

II. Soliton Systems

An important class of solutions to certain nonlinear evolution equations are traveling wave solutions that propagate with constant shape and velocity; these are referred to as "solitary waves." Specifically, a solitary wave solution with temporal and spatial variables t and n is a traveling wave of the form $u(n,t) = f(n-ct) = f(z)$, where c is a fixed constant, and the energy of $f(z)$ is localized in z. The Toda lattice

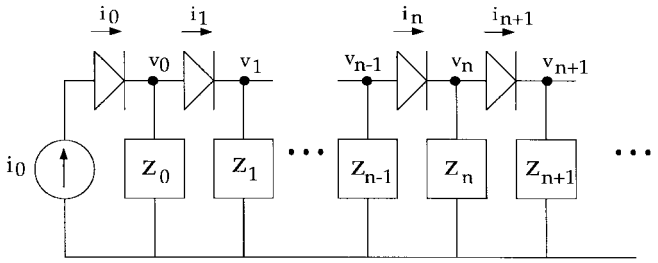

Fig. 1. Diode ladder network.

equations describe one such nonlinear system that possesses solitary wave solutions.

Originally developed to describe a nonlinear spring mass system [16], the Toda lattice equations govern the dynamics of the diode ladder network shown in Fig. 1, where each of the shunt impedances is a double capacitor, i.e., $Z_n = \alpha/s^2$ [14]. In terms of the voltages across the double capacitors v_n, the Toda lattice equations are

$$\frac{d^2 v_n(t)}{dt^2} = \alpha I_s(\exp\{(v_{n-1}(t) - v_n(t))/v_t\} - \exp\{(v_n(t) - v_{n+1}(t))/v_t\}) \quad (1)$$

or, equivalently, in terms of the diode currents

$$\frac{d^2}{dt^2}\ln\left(1 + \frac{i_n(t)}{I_s}\right) = \frac{\alpha}{v_t}(i_{n-1}(t) - 2i_n(t) + i_{n+1}(t)) \quad (2)$$

where

I_s saturation current in the diodes;
v_t thermal voltage;
$i_n(t)$ current through the nth diode.

This set of ordinary differential equations describes the behavior of the cascade system, whose dynamics can be completely specified by the one-dimensional (1-D) signal $i_0(t)$. When $i_0(t)$ in Fig. 1 is of the form

$$i_0(t) = \beta^2 \operatorname{sech}^2(\beta\tau) \quad (3)$$

the response of the diode ladder circuit is

$$i_n(t) = \beta^2 \operatorname{sech}^2(pn - \beta\tau) \quad (4)$$

where $\beta = \sqrt{I_s}\sinh(p)$, and $\tau = t\sqrt{\alpha/v_t}$.

The relationship between the amplitude, velocity, and effective pulse-width of these waves leads to narrower waves that are larger in amplitude, which will propagate faster than wider waves that are smaller in amplitude. If a solution to the equation is composed of solitary waves with different amplitudes, then collisions between the solitary waves are possible. The term "soliton" refers to such solitary wave solutions that retain their identity on collision with other solitary waves. As the individual solitary waves approach one another, they begin to interact nonlinearly. However, after passing through one another, they regain their shape and speed with only a slight positional shift [17].

There are many physical systems that support soliton solutions in a wide range of media [1], [3], [5], [9]. These can be distributed systems with dynamics described by partial differential equations and whose solitons propagate through a

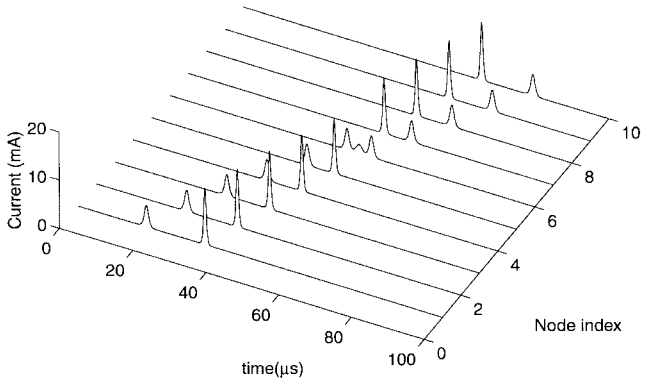

Fig. 2. Two solitary wave solutions to the Toda lattice.

bulk medium such as water, optical fiber, or plasma. They can also be lumped or cascade systems in which solitons propagate along a chain of identical nodes, such as in a crystal lattice, a nonlinear ladder network, or a metallic-grating surface acoustic wave device. These cascade soliton systems, such as the Toda lattice, are often described by systems of ordinary rather than partial differential equations.

Fig. 2 illustrates soliton behavior in the Toda lattice for two solutions of the form of (4). Each trace in the figure corresponds to the current in the diode at the associated index. As shown in the figure, the Toda lattice exhibits the key features of soliton behavior previously mentioned. This one-parameter family of solutions has an amplitude-dependent velocity with which it passes through the circuit. As the larger soliton catches up to the smaller soliton, as viewed on the sixth node, the combined amplitude of the two solitons is actually less than would result from a linear superposition of the two amplitudes. In addition, the signal shape changes significantly during this nonlinear interaction. Each of these characteristics of soliton interaction has useful implications in the communications context developed in this paper.

A well-known and often defining property of soliton systems is that by means of the inverse scattering transform, they can be described by an equivalent representation through the evolution of a specific linear operator whose eigenvalues remain constant with time. Specifically, soliton systems possess a symmetric linear operator $L(t)$ whose temporal evolution satisfies an operator differential equation of the form

$$\frac{dL(t)}{dt} = B(t)L(t) - L(t)B(t) \tag{5}$$

where $B(t)$ is an antisymmetric linear operator, and the nonlinear evolution equation is implicitly determined by (5). For example, the Toda lattice equations can be expressed in this form, where the elements of a matrix $L(t)$ describe the voltages at nodes in the lattice. In this representation, solitons present in the system correspond to eigenvalues in the discrete spectrum of the linear operator $L(t)$. The dynamics of solitons that correspond to different eigenvalues are uncoupled. However, their contributions to the solution in the observed system are nonlinearly coupled. Through a process called "inverse scattering," the state of the system at any time

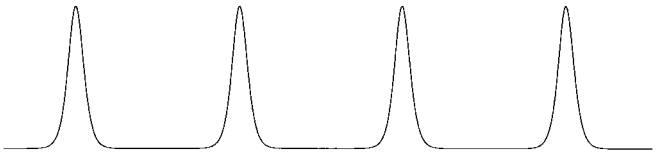

Fig. 3. Soliton carrier signal.

can be completely reconstructed from the eigenvalues and eigenfunctions of $L(0)$. A detailed treatment of the inverse scattering method can be found in [1].

For the Toda lattice, $L(t)$ and $B(t)$ are the symmetric and antisymmetric tridiagonal matrices given by

$$L = \begin{bmatrix} \ddots & a_{n-1} & \\ a_{n-1} & b_n & a_n \\ & a_n & \ddots \end{bmatrix}$$

$$B = \begin{bmatrix} \ddots & -a_{n-1} & \\ a_{n-1} & 0 & -a_n \\ & a_n & \ddots \end{bmatrix} \tag{6}$$

where $a_n = \exp\{(v_n - v_{n+1})/2\}/2$, $b_n = \dot{v}_n/2$ for voltages v_n in a solution to (1). When written in this form, (5) implicitly contains the Toda lattice equations. Although each of the entries of $L(t)$ evolve with time, the eigenvalues of $L(t)$ remain constant.

If the motion on the lattice is confined to a finite region of the lattice, i.e., the lattice is at rest for $|n| \to \infty$, then the spectrum of eigenvalues for the matrix $L(t)$ can be separated into two sets. There is a continuum of eigenvalues $\lambda \in [-1, 1]$ and a discrete set of eigenvalues for which $|\lambda_k| > 1$. When the lattice is at rest, the eigenvalues consist only of the continuum. When there are solitons in the lattice, one discrete eigenvalue will be present for each soliton excited. This separation of eigenvalues of $L(t)$ into discrete and continuous components is common to all of the soliton systems solved with inverse scattering. A more detailed investigation of the inverse scattering method as applied to the Toda lattice can be found in [16].

III. Soliton Modulation and Multiplexing Strategies

To explore some of the properties of the soliton signals generated by nonlinear systems as described in Section II, we propose a simplified example of a multiplexed communication system. By using solitons as carriers that can be independently modulated and multiplexed by the underlying nonlinear systems, the problems of detection and parameter estimation of soliton signals can be related to aspects of performance of the communication system. In this section, we outline the modulation and multiplexing strategy, highlighting the basic ideas without focusing on the detailed system implementation.

In order to use soliton signals as carriers of information, we define a soliton carrier as a periodic soliton signal that has one or more solitons of different parameter values contained within each period. As an example, a soliton carrier with one soliton in each period is depicted in Fig. 3. Information can

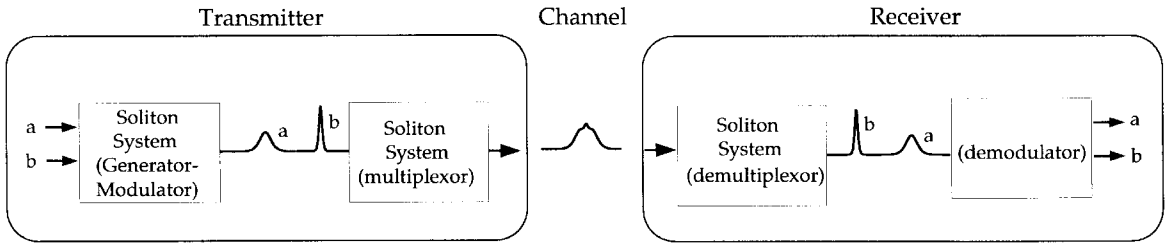

Fig. 4. Multiplexed soliton communication system. The transmitter generates a multisoliton carrier whose parameters are each modulated with different message streams. The multisoliton signal is then multiplexed by the nonlinear system in preparation for transmission over an identity channel. At the receiver, the signal is again passed through the nonlinear system to demultiplex the individual message streams.

be embedded in the parameters of the solitons, which will either affect the shape or relative spacing of the solitons in each period.

In Section II, it was demonstrated that solitons of different parameter values approach and pass through one another as the signal is processed by the nonlinear system. By passing a soliton carrier through a section of the nonlinear system of just the right length, the component solitons in each period of the carrier signal will superimpose; the effect of passing the carrier through the nonlinear system will be to multiplex the component solitons such that they become coincidental in time. If the signal is extracted from the nonlinear system at this point, the multiplexed solitons will remain "frozen" in their current relative positions. At a later point in time, this multiplexed waveform could be demultiplexed by continuing the process. By passing the signal through an equivalent length section of the nonlinear system, the component solitons will finish passing through one another, leaving the carrier once again with multiple nonoverlapping solitons.

By combining the notions of modulating soliton carriers with multiplexing the component solitons within each period, a simple multiplexed communication system can be constructed. The overall process is depicted in Fig. 4. Specifically, the transmitter takes as input several message streams, which it uses to generate a multisoliton carrier signal whose parameters are each modulated by a corresponding message stream. In the example shown in the figure, this signal consists of two solitons, where the smaller soliton is modulated by stream a and the larger by b. The modulated soliton carrier is then passed through an appropriate length section of the nonlinear system, which acts as a multiplexor, combining the solitons in time. The output of the multiplexor is a packetized soliton carrier, whose solitons remain fixed in their relative locations since they no longer evolve according to the nonlinear system dynamics.

The output of the transmitter is then sent over a channel. When the channel is an identity channel, the receiver can use a nonlinear system identical to that used for multiplexing to continue the nonlinear evolution of the solitons and thus separate out the component solitons in each period. Each of the individual message streams can then be recovered independently. In order to further develop some of the ideas of soliton carrier modulation and multiplexing, for the remainder of this paper, we focus our attention on one specific class of nonlinear systems: those governed by the Toda lattice equations.

IV. Toda Lattice Soliton Modulation and Multiplexing

The cascade structure of the Toda lattice system enables a convenient implementation of the modulation and multiplexing ideas of Section III. A periodic soliton carrier signal for the Toda lattice of the form depicted in Fig. 3 can be written as a sum of solutions of the form (4), i.e.,

$$i_n(t) = \sum_{\ell=-\infty}^{\infty} \beta^2 \operatorname{sech}^2[\alpha(n-\lambda\ell) - \beta t] - 2\beta. \qquad (7)$$

Modulating the parameter β or the relative positions of the solitons in each period results in a form of scale modulation or pulse-position modulation.

A multisoliton example is shown in Fig. 5 for a four-soliton signal using the Toda lattice circuits developed in [14]. In order for the circuits to act as multiplexors, the carrier signal is a periodically repeated train of four solitons of increasing parameter β. As such, this system could support four separate information streams: one on each of the component solitons.

Although presented in the context of the Toda lattice equation, as indicated at the outset of the paper, the soliton modulation techniques developed here are applicable to a variety of soliton systems, both in discrete and continuous time. For example, a similar technique can be used for modulation of the discrete-time solitons generated by the discrete-KdV equation whose circuit implementation is discussed in [14]. Related techniques for modulation of information on soliton carriers were previously proposed by Hirota *et al.* [18], [19]. Although their signal generation and processing methods relied on an inexact phenomenon known as "recurrence," the modulation paradigm they presented is essentially a two-soliton version of the carrier modulation paradigm presented here. However, the methods used to generate and multiplex solitons required extremely long lattices for only two solitons and required a specific relationship between the soliton amplitudes. Unlike the methods presented here, such methods do not generalize to an arbitrary number of solitons with arbitrary parameters. Further, the number of nodes in the lattice would increase exponentially with the number of solitons for the restricted set of parameters that could be accommodated.

A. Fourier Spectrum of Toda Lattice Solitons

The soliton demodulation and demultiplexing techniques discussed in this paper assume that there is no convolutional

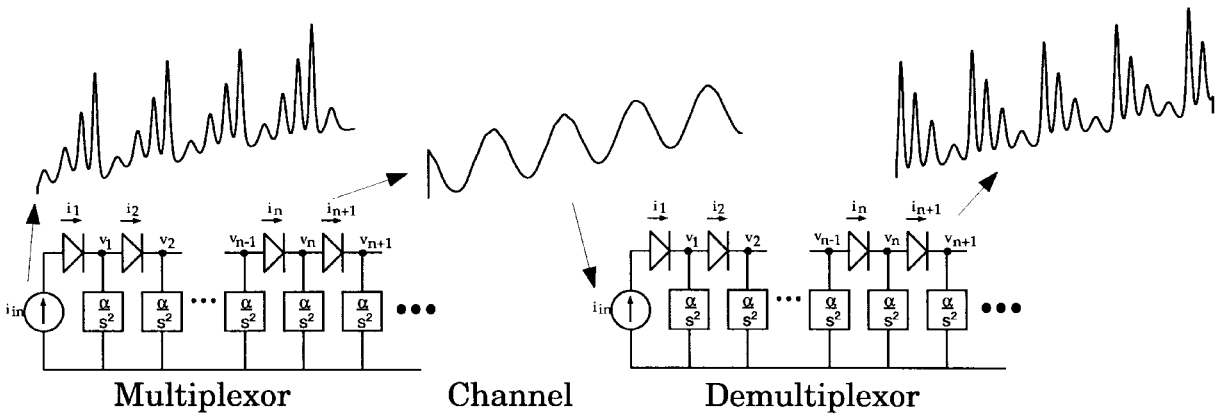

Fig. 5. Multiplexing of a four soliton solution to the Toda lattice.

distortion in the received signal, which is the case when the bandwidth of the soliton signals is small compared with the available channel bandwidth, i.e., the channel bandwidth is sufficiently wide (frequency nonselective) to pass the soliton without distortion. We assess the bandwidth requirements by exploring the spectral characteristics of multisoliton signals. A periodic single soliton carrier for the Toda lattice of the form (7) at a fixed node

$$f(t) = \sum_{\ell=-\infty}^{\infty} \beta^2 \operatorname{sech}^2(\beta(t - \ell T)) - 2\beta \tag{8}$$

where T is the period of the carrier, has a Fourier transform given by

$$F(\omega) = \omega_c \sum_{\ell=-\infty,\, \ell\neq 0}^{\infty} \frac{\pi\omega}{\sinh(\pi\omega/2\beta)}\, \delta(\omega - \ell\omega_c) \tag{9}$$

where $\omega_c = 2\pi/T$, resulting in Fourier series coefficients that fall off exponentially in frequency.

A single period of the two-soliton signal can be written [6]

$$f(t) = \frac{\beta_1^2 \operatorname{sech}^2(\eta_1) + \beta_2^2 \operatorname{sech}^2(\eta_2) + A \operatorname{sech}^2(\eta_1) \operatorname{sech}^2(\eta_2)}{(\cosh(\phi/2) + \sinh(\phi/2)\, \tanh(\eta_1)\, \tanh(\eta_2))^2} \tag{10}$$

with $\eta_i = \beta_i(t - \delta_i)$. When the solitons do not overlap in time, $A \approx 0$, and the denominator in (10) is approximately unity; therefore, the modulation is essentially the sum of the individually modulated waveforms. As the solitons begin to overlap, the contribution from the multiplicative cross term becomes significant, and spectral mixing of the component messages will occur. This results in bandwidth expansion of the multisoliton signal due to the convolution of the spectra of each of the component solitons.

B. Low-Energy Signaling with Soliton Signals

As depicted in Figs. 2 and 6, there is a net reduction of signal amplitude as multiple Toda lattice solitons interact. As mentioned in Section I, this nonlinear coupling among the component solitons can be exploited to yield a reduction in the energy required to transmit the soliton carrier.

In fact, for a two-soliton carrier, as a function of the relative separation of the two solitons, the energy of the transmitted signal is minimized precisely at the point of overlap. This is shown in the Appendix by analysis of the energy that would be required to transmit the waveform $v(t;\, \delta_1,\, \delta_2) = f_n(t)$ in (10)

$$E = \int_{-\infty}^{\infty} v(t;\, \delta_1,\, \delta_2)^2\, dt. \tag{11}$$

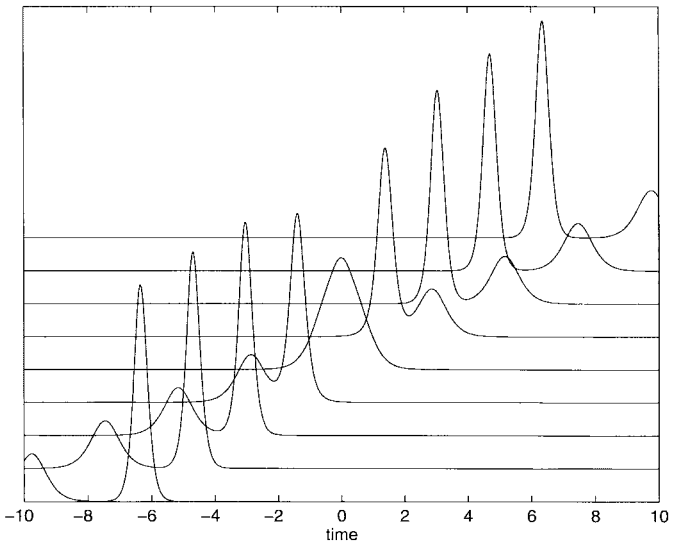

Fig. 6. Two-soliton solution is depicted in the Toda lattice. Each horizontal trace is the response at a successive node in the lattice. In this case, the two soliton wavenumbers are $p_1 = 2$ and $p_2 = 1.3$.

As shown in Fig. 6, when the two solitons are well separated in time, $|\delta_1 - \delta_2| \gg 0$, and the two component solitons are each distinguishable. In this case, $A \approx 0$, and the denominator is approximately unity in (10). However, as the solitons come to interact, $\delta_1 \approx \delta_2$, the nonlinear cross term and the denominator in (10) become significant, and the combined signal amplitude decreases.

The resulting effect on the energy of the signal is illustrated in Fig. 7 for several different values of the parameter β_2 holding β_1 fixed and with $\beta_2 < \beta_1$. Significant energy reduction occurs for a fairly wide range of separations $\delta_1 - \delta_2$, indicating that the modulation techniques described in this section could take advantage of this reduction, even though modulation would cause the relative separation to deviate from $\delta_1 = \delta_2$. For example, for $\beta_2 = \sinh(1.25)$, $\beta_1 = \sinh(2)$, the

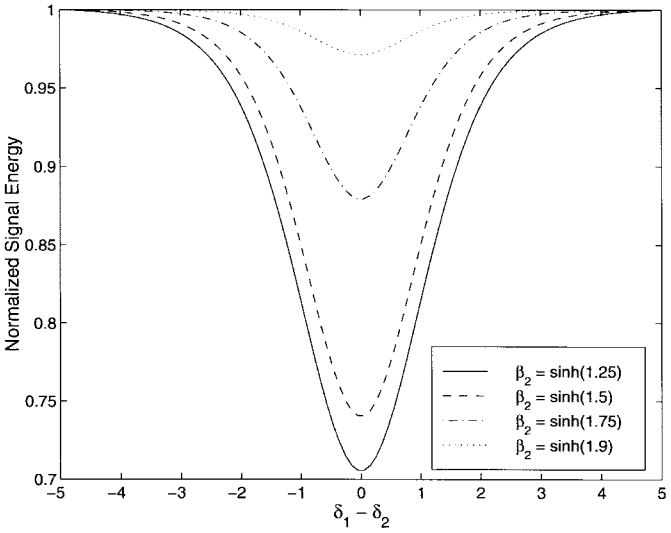

Fig. 7. Normalized signal energy for a two-soliton solution to the Toda lattice holding $\beta_1 = \sinh(2)$ fixed for three values of β_2. The signal energy is normalized by the maximum signal energy of the separated solitons.

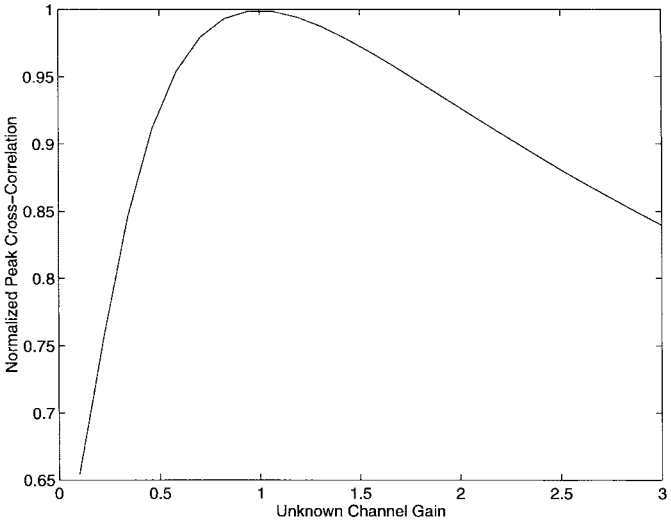

Fig. 8. Normalized cross-covariance of the input and output signals as a function of composite gain γ_c.

relative positions of the two solitons could be modulated by as much as ± 1.0 while still providing an energy reduction in excess of 20%. The nominal separation for these solitons in a two-soliton periodic carrier could be as small as 1.5 for the solitons to be essentially uncoupled. This would correspond to an "effective modulation depth" of 1.0/1.5 or 67% while maintaining 67% of the energy reduction available. If the multiplexed soliton system were used over an SNR-limited channel, then rather than transmitting the energy-reduced signal, the multisoliton signal could be rescaled to achieve the same SNR over the channel as the separated soliton signal. As we shall see, this has an overall effect of decreasing parameter estimation error at this fixed SNR.

V. Channel Effects

In our preliminary development, the multiplexing and communication contexts described in Sections III and IV considered an identity channel, allowing demultiplexing of the component streams at a receiver by simply processing a received multisoliton waveform with the Toda lattice equations. If these techniques were to be applied in more realistic channels, the multiplexed soliton waveform could undergo significant distortion from transmitter to receiver. In Section V-B, we consider effects of additive noise. In the following section, the issue of unknown channel gain is considered.

A. Gain Normalization

In any practical communication context, a modulation system must be able to combat the presence of an unknown gain due to channel fluctuations. This is a potential drawback of using Toda lattice solitons as carrier signals since these solitons have a specific relationship between the amplitude and pulse width. If the soliton signal $s(t) = \beta^2 \operatorname{sech}^2(\beta t)$ is transmitted through a channel and arrives at the receiver with an unknown gain $r(t) = \gamma s(t)$, then the soliton dynamics of the signal $s(t)$ can no longer be observed from processing the signal $r(t)$ directly with the Toda lattice. In general, the signal $r(t)$ will give rise to both soliton and nonsoliton components, where the soliton component may be of a different soliton parameter.

Many communication systems combat gain fluctuations with automatic gain control (AGC) to dynamically adjust the gain of a preamplifier in the receiver. To demonstrate the feasibility of AGC for the soliton modulation systems, we consider the effect of an unknown gain on a single soliton processed by the Toda lattice. Since processing the soliton will correspond to a simple time delay only when the unknown gain has been corrected, an AGC system might exploit differences between the input and the processed waveforms and adjust the gain until the processed waveform is a pure time delay of the input. As an example, in Fig. 8, the peak of the cross-covariance between the gain-adjusted soliton signal and the processed signal at the nth node of the lattice is shown as a function of the composite unknown gain γ_c. For this example, $\beta = \sinh(2)$, and $0.1 \leq \gamma_c \leq 3$. As shown, the normalized cross covariance has a unique maximum of $C = 1$ when the input to the Toda lattice has been properly rescaled, i.e., $\gamma_c = 1$. This gives an indication that AGC techniques based on feedback of the processed signal can be effective in combating unknown channel gain. However, a variety of issues including how such AGC might be performed for multisoliton signals or modulated multisoliton carriers remains unexplored.

B. Noise Dynamics in Soliton Systems

For even a simple additive noise channel, it is not clear that processing the received multisoliton waveform with the nonlinear evolution equations is an effective means of demultiplexing. In order to assess the degree to which a receiver can demultiplex and demodulate multisoliton signals in noise, it is necessary to first examine both the dynamics of the noise as it is processed and its effects on the soliton dynamics.

For the remainder of this paper, we assume an additive white Gaussian noise channel from transmitter to receiver, i.e., $r(t) = s(t) + n(t)$, where $s(t)$ is the multisoliton signal, and $n(t)$ is stationary white Gaussian noise. There are two

significant effects of the additive noise on the output of the receiver. First, when the received signal $r(t)$ is used as the input to the Toda lattice, then the noise from the channel has a dynamical effect on the solution to the Toda lattice. Our initial analysis of these dynamical effects in [14] focused primarily on the noise component while assuming that at high SNR, the soliton dynamics were unaffected. However, even at high SNR, the additive noise may also have an effect on the actual solitons excited in the lattice. Accordingly, we extend these results in our subsequent analysis developed in this paper, where inverse scattering techniques are used to examine the effects of additive noise on the induced soliton eigenvalues. The results we obtain are important both in developing an understanding of the temporal behavior of the soliton component of the signal and in determining the performance of any parameter estimation algorithms that employ inverse scattering.

As developed in [14], the dynamics of the Toda lattice equations when driven by white Gaussian noise with low noise power leads to a model in which an input–output relationship from the signal at the zeroth node to the output at the Nth node has the approximate frequency response

$$H_N(j\omega) = \begin{cases} e^{-2j\,\sin^{-1}(\omega_c)N}, & |\omega| < \omega_c \\ e^{[j\pi - 2\,\cosh^{-1}(\omega_c)]N}, & \text{otherwise} \end{cases} \tag{12}$$

where $\omega_c = \alpha/I_s v_t$. The lattice behaves like a lowpass filter and, for $N \gg 1$, approaches the ideal filter

$$|H_N(j\omega)|^2 \approx \begin{cases} 1, & |\omega| < \omega_c \\ 0, & \text{otherwise.} \end{cases} \tag{13}$$

These results are assumed to hold when soliton signals are also present in the input. Specifically, at high SNR, it is assumed that the soliton components are processed independently from the noise and that the noise is still effectively lowpass filtered. The validity of these assumptions was verified in [14] through both linearized analyses and simulation.

We next consider a complimentary noise model based on inverse scattering. As described in Section II, the inverse scattering transform provides a particularly useful mechanism for exploring the long-term behavior of soliton systems. In a manner similar to the use of the Fourier transform for describing the ability of linear processors to extract a signal from a stationary random background, the eigenvalues from inverse scattering can effectively characterize the ability of the system to extract the component solitons of a received soliton signal in noise, as we now develop.

To begin, recall that the dynamics of the Toda lattice may be described by the evolution of the matrix $L(t)$ given in (6), whose eigenvalues outside $|\lambda| \leq 1$ correspond to solitons. By considering the effects of small amplitude perturbations to the entries $a_n(t)$ and $b_n(t)$ on the eigenvalues of $L(t)$, we can observe the effects on the soliton dynamics through the corresponding eigenvalues.

Following [20], we write the $N \times N$ matrix L in the form $L = L_0 + D$, where L_0 is the unperturbed symmetric matrix corresponding to the noise-free soliton signal, and D is the symmetric random perturbation resulting from additive noise. By expanding the eigenvalues of the matrix L in a convergent series, we obtain [20],

$$\lambda_g = \mu_g + \hat{d}_{gg} - \sum_{i=1,\, i\neq g}^{N} \frac{\hat{d}_{gi}\hat{d}_{ig}}{\mu_{ig}} + \cdots \tag{14}$$

where μ_g is the gth eigenvalue of L_0, $\mu_{ig} = \mu_i - \mu_g$, and $\hat{d}_{ij}$ are the elements of the matrix $\hat{D}$ defined by $\hat{D} = C^{\top} D C$, where C diagonalizes L_0.

Since $E\{\hat{d}_{gg}\} = 0$, then to first order in the elements of D, the eigenvalues of L are unbiased estimates of the eigenvalues of L_0. In addition, since $\hat{d}_{gg}$ is a linear combination of the elements of D, then if the elements of D are jointly Gaussian, which is a reasonable assumption at high SNR; then, to first order, the eigenvalues of L will be jointly Gaussian, distributed about the eigenvalues of L_0.

The proceeding leads to some important interpretations. When processing small amplitude white Gaussian noise alone, the lattice can be viewed as a dispersive lowpass filter; therefore, the output of the system will approximately be bandlimited white Gaussian noise at each node. In the presence of noise, solitons will be essentially unperturbed, and the noise will remain Gaussian and bandlimited. Via inverse scattering, to first order, small amplitude noise alone only excites eigenvalues corresponding to the nonsoliton continuum. When solitons are also processed, the noise induces a small Gaussian perturbation to the true soliton eigenvalues as well. These properties are exploited in the next two sections, which consider estimation and detection of soliton signals.

VI. Estimation of Soliton Signals

In physical or natural systems, it is often necessary to estimate solitons or their parameters from measurements. This is the case, for example, when they are masked by external noise in the measurements or by strong nonsoliton components or when many solitons are superimposed, making them difficult to resolve. These situations can all arise in the communication techniques suggested in Sections III and IV. In this section, we explore soliton parameter estimation by investigating the ability of a receiver to estimate the parameters of the multisoliton carrier from corrupted measurements.

We first determine bounds on the performance of any unbiased estimator of the scale parameters β_i and the relative positions δ_i of multisoliton signals in stationary white Gaussian noise with noise power N_0. A bound on the variance of an estimate of the parameter β may be useful in determining the demodulation performance of a parameter modulation system, where the component soliton wavenumbers are slightly modulated. When $s(t)$ contains two solitons that are separated in time and therefore are not interacting, the multisoliton signal appears as a linear superposition of the two, i.e.,

$$\begin{aligned} s(t) &\approx \beta_1^2\,\mathrm{sech}^2(\beta_1(t-\delta_1)) + \beta_1^2\,\mathrm{sech}^2(\beta_2(t-\delta_2)) \\ &= s_1(t) + s_2(t). \end{aligned} \tag{15}$$

As such, each of the component solitons can be treated separately. As we shall see, for large separations, the ability to estimate the parameters β_1 and β_2 from $s(t)$ is the same as estimating β_1 from $s_1(t)$ and β_2 from $s_2(t)$, respectively.

If the time locations of each soliton are known, then the variance of any unbiased estimator $\hat{\beta}_i$ of β_i must satisfy the Cramér–Rao lower bound [21]

$$\mathrm{Var}(\hat{\beta}) \geq \frac{N_0}{\displaystyle\int_{t_i}^{t_f} \left(\frac{\partial s_i(t;\beta)}{\partial \beta}\right)^2 dt}. \tag{16}$$

For the infinite observation interval $-\infty < t < \infty$, the Cramér–Rao Bound (16) can be evaluated to be [13]

$$\mathrm{Var}(\hat{\beta}) \geq \frac{N_0}{\left(\dfrac{8}{3}+\dfrac{4\pi^2}{45}\right)\beta} \approx \frac{N_0}{3.544\beta}. \tag{17}$$

A Cramér–Rao bound would also be useful for determining the demodulation performance of pulse position modulation, where the soliton position is slightly modulated. For each of the separated solitons, $s_i(t) = \beta_i^2 \operatorname{sech}^2(\beta_i(t-\delta_i))$, where δ_i is the relative position of the soliton in a period of the carrier, the Cramér–Rao bound for $\hat{\delta}$ is given by

$$\begin{aligned}\mathrm{Var}(\hat{\delta}) &\geq \frac{N_0}{\displaystyle\int_{t_i}^{t_f} 4\beta^6 \operatorname{sech}^4(\beta(t-\delta))\, \tanh^2(\beta(t-\delta))\, dt} \\ &= \frac{N_0}{\left(\dfrac{16}{15}\right)\beta^5}.\end{aligned} \tag{18}$$

More generally, when the received signal is a multisoliton waveform where the solitons are multiplexed in time, the signal shape is sensitive to the relative positions of the solitons, and parameter estimation becomes more difficult. We will focus our attention on the two-soliton solution to the Toda lattice

$$s(t) = \frac{\beta_1^2 \operatorname{sech}^2(\eta_1) + \beta_2^2 \operatorname{sech}^2(\eta_2) + A \operatorname{sech}^2(\eta_1)\operatorname{sech}^2(\eta_2)}{(\cosh(\phi/2) + \sinh(\phi/2)\, \tanh(\eta_1)\, \tanh(\eta_2))^2} \tag{19}$$

where

$$A = \sinh(\phi/2)((\beta_1^2+\beta_2^2)\, \sinh(\phi/2) + 2\beta_1\beta_2\, \cosh(\phi/2)) \tag{20}$$

with both solitons traveling in the same direction and with $\beta_1 > \beta_2$,

$$\phi = \ln\left(\frac{\sinh((p_1-p_2)/2)}{\sinh((p_1+p_2)/2)}\right) \tag{21}$$

where $\beta_i = \sinh(p_i)$, and $\eta_i = \beta_i(t-\delta_i)$.

In the communication context, we are generally interested in parameter estimation with an unknown relative spacing among the solitons. Either the relative spacing of the solitons has been modulated and is therefore unknown to the receiver, or the parameters β_1 and β_2 are modulated, and the induced phase shift in the received solitons ϕ is unknown. In either case, the Cramér–Rao bound for jointly estimating the parameters of a multisoliton signal from observations of $r(t)$ can be obtained numerically by forming the Fisher information matrix $I(\Theta)$, where $\Theta = [\delta_1, \delta_2, \beta_1, \beta_2]^\top$

$$[I(\Theta)]_{i,j} = \frac{1}{N_0}\int_{t_i}^{t_f} \left(\frac{\partial s(t;\Theta)}{\partial \Theta_i}\, \frac{\partial s(t;\Theta)}{\partial \Theta_j}\right) dt \tag{22}$$

where Θ_i is the ith element of Θ. The usual resulting bound on the estimation variance for parameter Θ_i is given by [21]

$$\mathrm{Var}(\hat{\Theta}_i) \geq [I^{-1}(\Theta)]_{ii}. \tag{23}$$

For large separations $\delta = \delta_1 - \delta_2$, the Cramér–Rao bound for estimating the parameters of either soliton will be unaffected by the parameters of the other. As shown in Fig. 9(a), when the component solitons are well separated, the bound for either β_1 or β_2 approaches the bound for estimation of a single soliton with that parameter value in the same level of noise. The bounds for estimating β_1 and β_2 are shown in Fig. 9(a) as a function of the relative separation, δ.

Note that both of the bounds are reduced by the nonlinear superposition, indicating that the potential performance of the receiver is enhanced by multiplexing. As was shown in Section IV-B, the energy of the signal is reduced by multiplexing, which indicates that this performance enhancement is achieved at a lower signal-to-noise ratio since the noise power was held fixed. However, as we let the parameter difference $\beta_2 - \beta_1$ increase, we notice a different character to the bounds. Note that in Fig. 9(b), the performance of the larger soliton is inhibited by the nonlinear superposition, whereas the smaller soliton is still enhanced. In fact, the bound for the smaller soliton becomes lower than that for the larger soliton near the range $\delta = 0$.

The ability to simultaneously enhance estimation performance while decreasing signal energy is an inherently nonlinear phenomena. Using (16), we obtain the familiar Cramér–Rao bound for linear estimation, which is inversely proportional to the signal energy

$$\begin{aligned}\mathrm{Var}(\hat{\beta}) &\geq \frac{N_0}{\displaystyle\int_{t_i}^{t_f} \left(\frac{\partial \beta s(t)}{\partial \beta}\right)^2 dt} \\ &= \frac{N_0}{\displaystyle\int_{t_i}^{t_f} s^2(t)\, dt} = \frac{1}{\mathrm{SNR}}.\end{aligned} \tag{24}$$

However, when the signal has a nonlinear dependence on the parameter, the bound is a function of the energy in the derivative of the signal with respect to the parameter rather

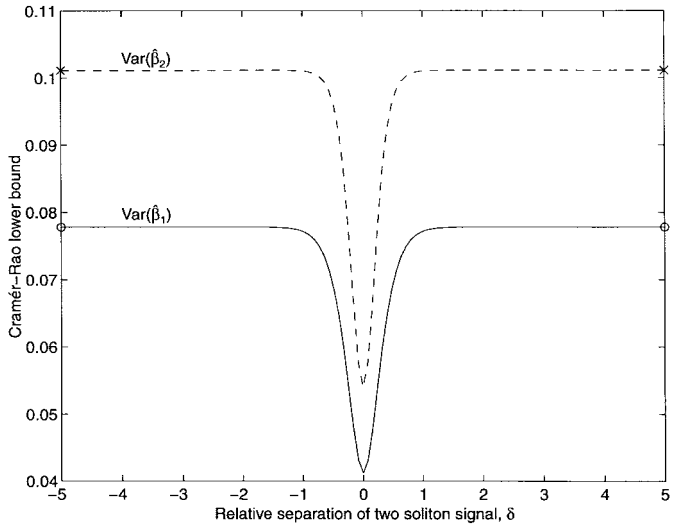

(a)

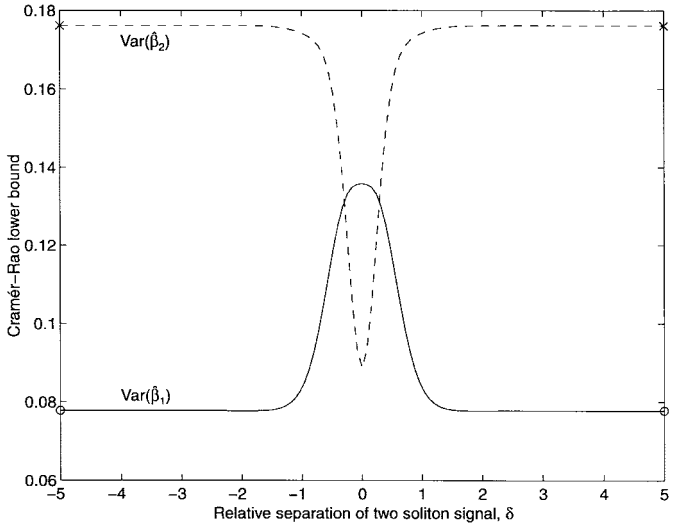

(b)

Fig. 9. Cramér–Rao lower bound for estimating β_1 and β_2 with all parameters unknown in white Gaussian noise with $N_0 = 1$. The bounds are shown as a function of the relative separation $\delta = \delta_1 - \delta_2$. The Cramér–Rao bound for estimating β_1 and β_2 of a single soliton with the same parameter value is indicated with "o" and "×" marks, respectively, as given by (17). (a) $\beta_1 = \sinh(2)$ and $\beta_2 = \sinh(1.75)$. (b) $\beta_1 = \sinh(2)$ and $\beta_2 = \sinh(1.25)$.

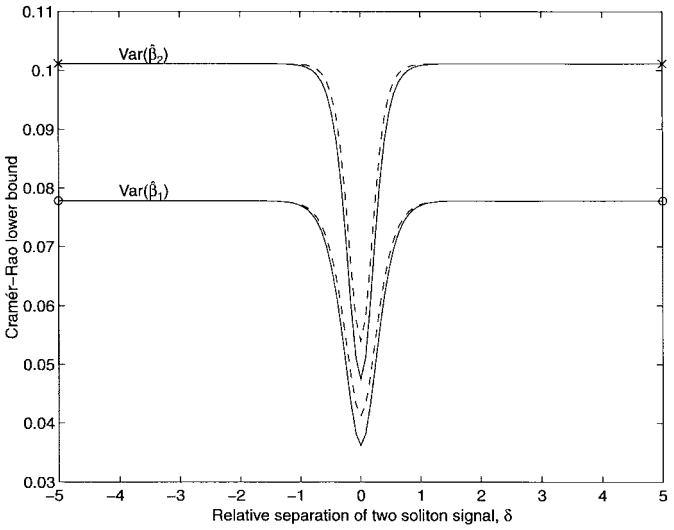

(a)

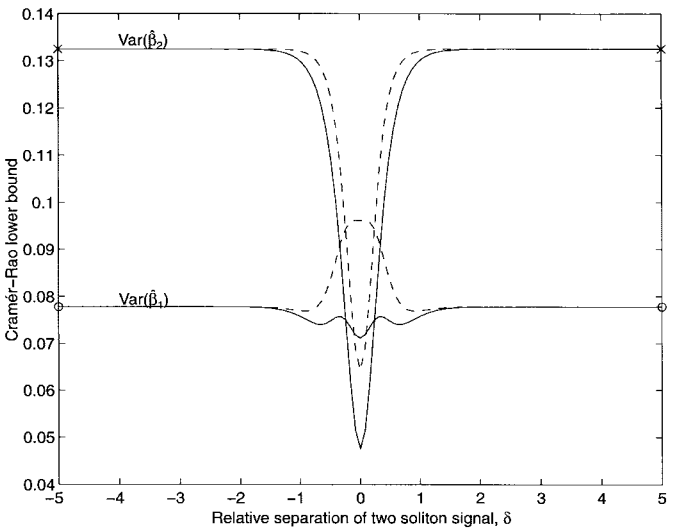

(b)

Fig. 10. Cramér–Rao lower bound for estimating β_1 and β_2 with all parameters unknown in white Gaussian noise. The bounds that result from multiplexing the solitons without signal rescaling are shown with dashed lines. The bounds that result from maintaining a constant SNR for all separations are shown with solid lines. (a) $\beta_1 = \sinh(2)$ and $\beta_2 = \sinh(1.75)$. (b) $\beta_1 = \sinh(2)$ and $\beta_2 = \sinh(1.5)$.

than signal energy. Bounds for estimating the times of arrival δ_i of the two component solitons can also be shown to agree with the single soliton bounds for large separations and are qualitatively similar to those for estimating the scaling parameters.

To illustrate the combined effects of the energy reduction and parameter estimation enhancement that occurs during multiplexing, in Fig. 10(a), the Cramér–Rao bounds are shown for a fixed SNR, rather than a fixed noise power N_0. If the transmitter were to send information embedded in the parameters β_i of a carrier with separated solitons at an SNR of about 19.7 dB, then the performance of the receiver would be bounded by the Cramér–Rao bounds for separated solitons, e.g., the points labeled "x" and "o" in Fig. 9(a) as given by (17). For this example, this corresponds to a mean-squared parameter estimation error of 0.1011 and 0.0778 or about 2.15% and 3.62%, respectively.

If the transmitter sent the same information embedded in the parameters but prior to transmission multiplexed the solitons using the Toda lattice, then the performance of the receiver would be bounded by the solid and dashed lines in Fig. 9(a). For this example, this corresponds to a mean-squared parameter estimation error of 0.0412 and 0.0540 or about 1.14% and 1.94%, respectively. This reduction in mean-squared parameter estimation error is a result of the increased sensitivity of the multiplexed soliton signal to the parameters and was accomplished with less transmitted signal power. If the SNR of the transmitted signal were the same for the multiplexed and separated signals, for this example, the resulting mean-squared parameter estimation error would

decrease even further to 0.0362 and 0.0475 or to 1.0% and 1.7%, respectively. This additional 14% reduction in parameter estimation error is due to the effective increase in available SNR, which is made possible by the reduction in energy of the multiplexed signal.

Fig. 10(a) and (b) explicitly show the mean-squared error reduction that results from boosting the SNR of the multiplexed signal to that of the separated solitons. The original Cramér–Rao bounds for each parameter are indicated using dashed lines and are the same as those in Fig. 9(a). The bounds that result from rescaling the multiplexed signal are indicated in solid lines and lie below the original bounds. To further illustrate the potential for exploiting the energy reduction, in Fig. 10(b), the same process was repeated for $\beta_1 = \sinh(2)$ and $\beta_1 = \sinh(1.5)$. Note that in this example, prior to energy normalization, the mean-squared estimation error for the larger soliton is increased from multiplexing. However, once the SNR of the multiplexed signal is brought to the same level as the separated solitons, the overall mean-squared estimation error for the larger soliton is reduced.

A. Estimation Based on Demultiplexing

In this section, we consider estimating the parameters of soliton signals by first demultiplexing and, therefore, decoupling the component solitons. Once separated, more conventional techniques can be applied to parameter estimation. The algorithms described are representative of the types of operations that might appear in a receiver for the communication techniques suggested in Sections III and IV. As such, the bounds presented in the previous section and the performance of the algorithms in this section should give some indication of potential receiver performance. As a model for the receiver structure, we will focus on the diode ladder circuit implementation of the Toda lattice equations (2), where $i_n(t)$ is the current through the nth diode $i_0(t) = r(t)$, and for simplicity, the parameters of all circuit elements have been normalized to unity.

When the component solitons in a multisoliton signal are separated in time, the positions of each of the solitons can be estimated independently. Consider estimating the position δ_i of one of the separated component solitons in a solution to (2)

$$s_i(t-\delta_i) = \beta_i^2 \operatorname{sech}^2(\beta_i(t-\delta_i)) \tag{25}$$

with the parameter β_i known. This is classical time-of-arrival estimation. For observations $r(t) = s_i(t) + n(t)$, where $n(t)$ is a stationary white Gaussian process, the familiar maximum likelihood estimate can be obtained through convolution with a matched filter followed by a peak detector [21].

When the signal $r(t)$ contains a multisoliton signal in which the solitons are multiplexed and overlapping in time, then the estimation of the vector of parameters $\underline{\delta}$ from the received signal $r(t) = s(t; \underline{\beta}, \underline{\delta}) + n(t)$ becomes more involved. If the component solitons are not well separated, their parameters are tightly coupled to the entire signal and should not be estimated independently. However, the parameters can be decoupled by preprocessing the signal $r(t)$ with the Toda lattice. By driving the Toda lattice with the received signal such that

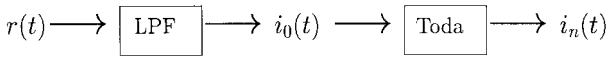

Fig. 11. Toda lattice receiver model.

$i_0(t) = r(t)$ in (2), then as the signal is processed by the lattice, the component solitons will naturally separate, owing to their different propagation velocities. This gives rise to the following strategy for estimating the positions of each of the multiplexed solitons: First, use the Toda lattice to separate each of the component solitons in time; then, estimate the positions of each of the separated solitons using a matched filter as before. By the invertibility of the Toda lattice equations, the ML estimate of the positions of the separated solitons are identical to those based on the received signal $r(t)$.

When the signal $r(t)$ is used to drive the lattice, each of the component solitons in $r(t)$ will propagate down the lattice appearing in the signal $i_k(t)$ at node k. For each signal $i_k(t)$ in the solution to the dynamic equations (2), there will be a contribution from both the signal component $s(t)$ giving rise to $s_k(t)$ and the noise component $n(t)$ giving rise to $n_k(t)$, i.e., $i_k(t) = s_k(t) + n_k(t)$, where $n_0(t)$ is the stationary white Gaussian noise process $n(t)$, and $s_0(t)$ is the multiplexed soliton signal $s(t)$. From our linear noise analyses, at high SNR, the noise component of the solution $n_k(t)$ is well approximated as bandlimited white Gaussian noise, whereas the signal component $s_k(t)$ propagates unaffected by the noise. If the component solitons of the signal $i_k(t)$ are well separated by the time they appear in the signal $i_N(t)$ at node N, then the ML estimate of the positions of each of the component solitons based on the signal $i_N(t)$ can be obtained by standard matched filtering. Not only are the position estimates equal to those that would be obtained directly from $r(t)$, but they are also much simpler to compute.

To examine empirically the performance of this approach, we consider soliton signals in white Gaussian noise with noise power N_0. Rather than using the circuit hardware that was developed and presented in [14], computer simulations are used for the experiments in this paper. These simulations are performed using a Runge–Kutta integration routine with a fixed step size Δ. Since the bandwidth limitations of the channel and receiver will restrict the possible range of parameters, and to simplify our simulations, we assume that the receiver is a lowpass filter followed by a Toda lattice circuit, as shown in Fig. 11. We also assume that the bandwidth $2\pi/\Delta$ of the lowpass filter in Fig. 11 is wide enough to pass the soliton components of $r(t)$ completely. The input to the Toda lattice circuit $i_0(t)$ then contains the soliton signal in bandlimited white Gaussian noise.

For the two-soliton signal in (19), if the component solitons are well separated as viewed on the Nth node of the Toda lattice, the signal appears to be a linear superposition of two solitons

$$\begin{aligned} i_N(t) \approx{}& \beta_1^2 \operatorname{sech}^2(\beta_1(t-\delta_1) - p_1 N - \phi/2) \\ &+ \beta_2^2 \operatorname{sech}^2(\beta_2(t-\delta_2) - p_2 N + \phi/2) \end{aligned} \tag{26}$$

where $\phi/2$ is the time-shift incurred due to the nonlinear interaction. Matched filters can now be used to estimate the

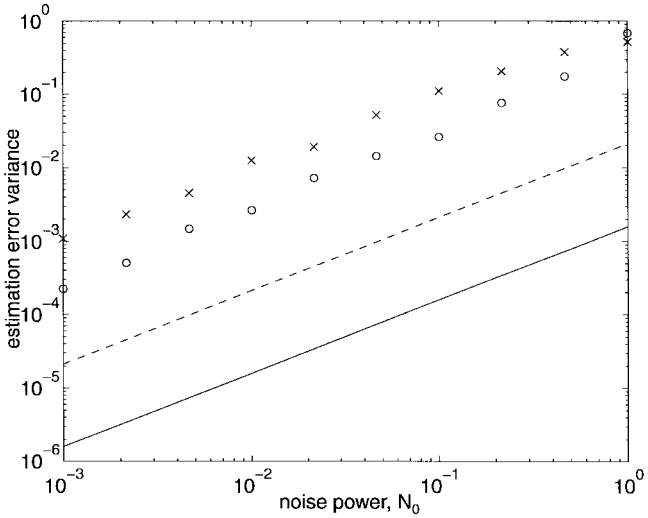

Fig. 12. Cramér–Rao bounds for δ_1 and δ_2 are shown with solid and dashed lines, whereas the estimation error results of 100 Monte Carlo trials are indicated with "o" and "×" marks, respectively.

time of the arrival of each soliton at the Nth node. We formulate the estimates

$$\hat{\delta}_1 = \left(t^a_{N,1} - \frac{p_1 N + \phi/2}{\beta_1} \right)$$
$$\hat{\delta}_2 = \left(t^a_{N,2} - \frac{p_2 N - \phi/2}{\beta_2} \right) \tag{27}$$

where $t^a_{N,i}$ is the time of arrival of the ith soliton and node N. The performance of this algorithm for a two-soliton signal with $\underline{\beta} = [\sinh(2), \sinh(1.5)]$ is shown in Fig. 12. Note that although the error variance of each estimate is apparently a constant multiple of the Cramér–Rao bound, the estimation error variance still approaches the bound in an absolute sense as $N_0 \rightarrow 0$.

The scaling parameters β_i can also be estimated by first demultiplexing the component solitons. In [13], an algorithm that uses velocity filtering techniques to estimate the parameters β_i of the separate solitons through their soliton velocities is presented and analyzed. The performance of such techniques is similar to that of the time-of-arrival estimation techniques, although this does not constitute an ML approach.

B. Estimation Based on Inverse Scattering

Because of the nonlinear manner in which the parameters β_i appear in a multisoliton signal, it is difficult to formulate an ML estimate directly from the received signal $r(t)$, even when the solitons are not multiplexed. However, we can use the inverse scattering framework along with some of the results from Section V-B to construct their ML estimates at high signal-to-noise ratios.

Since the transformation from the signal $r(t)$ to the eigenvalue-eigenvector representation of the inverse scattering transform is invertible, then ML estimates of the parameters β_i can be formulated using this representation. The matrix $L(t)$ and its inverse scattering decomposition can be obtained from the signal $r(t)$ by first driving the lattice with the signal and then sampling the circuit waveforms to construct $L(t)$ at a fixed time.

If the current at each node evolves according to the Toda lattice equations, then the eigenvalues of the matrix $L(t)$ are time invariant, and the eigenvalues for which $|\lambda_i| > 1$ correspond to soliton solutions, with $\beta_i = \sinh(\cosh^{-1}(\lambda_i)) = \sqrt{\lambda_i^2 - 1}$. In Section V-B, it was shown that in additive noise at high SNR, the eigenvalues of $L(t)$ are, to first order, jointly Gaussian and distributed about the true eigenvalues of the original multisoliton signal. Therefore, the eigenvalues of the matrix $L(t)$ generated from $r(t)$ constitute ML estimates of the underlying eigenvalues. ML estimates of the parameters β_i can be obtained through the one-to-one mapping from λ_i to β_i, $\hat{\beta}_i = \sinh(\cosh^{-1}(\lambda_i))$.

In order to perform eigenvalue estimation, the finite length of a practical implementation of the Toda lattice must be appropriately accommodated. This can be resolved by either using the periodic Jacoby matrix $L(t)$ that results from making the periodic assumption $a_N(t) = a_0(t)$ or by simply truncating the matrix. It can be shown that for the periodic Toda lattice, the eigenvalues of the periodic Jacoby matrix are also time invariant and correspond to periodic soliton solutions [4]. An example of the joint estimation of the parameters of a two-soliton signal is shown in Fig. 13(a). The estimation error variance decreases with the noise power at the same exponential rate as the Cramér–Rao bound.

To verify that the performance of the estimation algorithm has the same dependence on the relative separation of solitons as previously indicated, the estimation error variance is also indicated in Fig. 13(b) versus the relative separation δ. In the figure, the mean-squared parameter estimation error for each of the parameters β_i are shown along with their corresponding Cramér–Rao bound. At least empirically, we see that the fidelity of the parameter estimates are indeed enhanced by multiplexing, even though this corresponds to a signal with lower observational SNR since the noise power N_0 was held fixed.

VII. Detection of Soliton Signals

The inherent difficulties that arise in estimating the parameters of soliton signals also make detecting solitons a difficult task. If the soliton multiplexing strategy described in Sections III and IV were used to send signals from a base station to many receivers, each of the receivers may need to identify whether or not the received signal contained any information directed to them. If their receivers were tuned to specific soliton parameter values, then they would first need to detect the presence of a soliton at the prescribed value prior to demodulation. This would correspond to detection of a single or of multiple solitons that have been multiplexed and received in additive noise.

Detection of either a single soliton or of a signal composed of multiple nonoverlapping solitons in additive white Gaussian noise falls within the context of classical detection. The optimal receiver for a variety of measures, including the Bayes or Neyman–Pearson criteria, involves a matched filter followed by the usual likelihood ratio test.

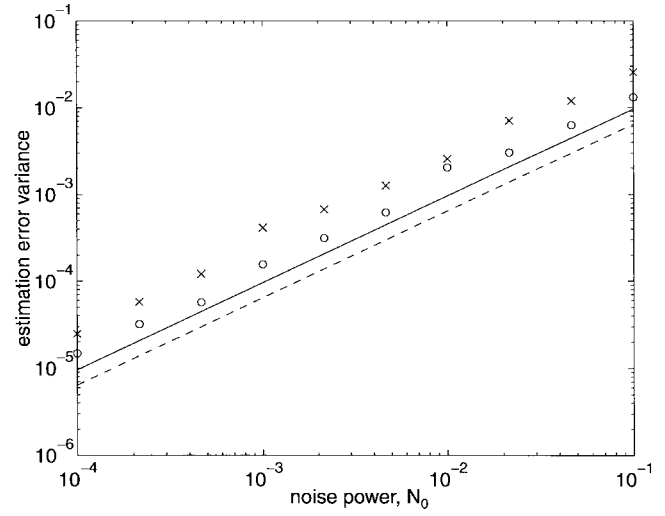

(a)

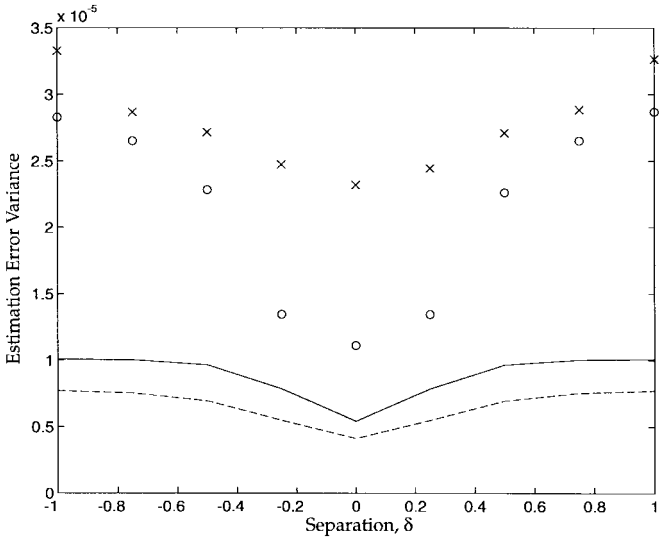

(b)

Fig. 13. Estimation error variance for the inverse scattering-based estimates of $\beta_1 = \sinh(2)$, $\beta_2 = \sinh(1.5)$. The bounds for β_1 and β_2 are indicated with solid and dashed lines, respectively. The estimation results for 100 Monte Carlo trials with a diode lattice of $N = 10$ nodes for β_1 and β_2 are indicated by the points labeled "o" and "×," respectively.

When the received signal $r(t)$ contains a multisoliton signal where the component solitons are multiplexed and not resolved, detection becomes more involved. Specifically, consider a two-soliton solution to the Toda lattice, where one of four decisions must be made.

1) Neither soliton is present.
2) Only soliton one is present.
3) Only soliton two is present.
4) Both solitons are present.

If the relative positions of the component solitons were known *a priori*, then detection reduces to deciding which one among four known signals is present. Once again, this falls within the scope of standard Gaussian detection theory.

If the relative positions of the solitons were unknown, as would be the case for a modulated soliton carrier, then the two-soliton signal $s_{12}(t)$ will vary significantly as a function of their relative separation, and the optimal processor is no longer a single matched filter. This leads to the composite hypothesis test

$$H_0\colon r(t) = n(t) \qquad H_2\colon r(t) = s_2(t;\, \delta_2) + n(t)$$
$$H_1\colon r(t) = s_1(t;\, \delta_1) + n(t), \quad H_{12}\colon r(t) = s_{12}(t;\, \underline{\delta}) + n(t)$$

where $s_1(t)$, $s_2(t)$, and $s_{12}(t)$ are soliton one, soliton two, and the two-soliton signals, respectively, and $\underline{\delta} = [\delta_1,\, \delta_2]^\top$, which usually results in a generalized likelihood ratio test.

Typically, when the waveform shape varies significantly as a function of the unknown parameter, multiple hypotheses are used with one for each value of the parameter sampled over a prespecified range. This is often the approach used for detection of a signal of unknown frequency or unknown spatial direction. For soliton detection, this approach would turn the current problem into one with hypotheses H_0, H_1, and H_2 as before, and an additional M hypotheses: one for each value of the parameter $\underline{\delta}$ sampled over a range of possible values. The resulting complexity increases exponentially with the number of component solitons N_s and requires a number of hypothesis tests given by

$$\sum_{i=1}^{N_s} \binom{N_s}{i} M^{i-1} = \frac{(M+1)^{N_s} - 1}{M} + 1. \tag{28}$$

However, as with parameter estimation in Section VI, multisoliton detection can be decoupled by demultiplexing the component solitons in the signal $r(t)$ with the Toda lattice. If the component solitons are separated as viewed on the Nth node, then detection can be more simply formulated using the signal $i_N(t)$. The invertibility of the lattice equations implies that a Bayes optimal decision based on $r(t)$ must be the same as that based on $i_N(t)$ since the likelihood function $\Lambda(r(t))$ and $\Lambda(i_N(t)) = \Lambda(T\{r(t)\})$ are identical for any invertible transformation $T\{\cdot\}$.

Although a generalized likelihood ratio test still must be used, where the value of $\hat{\underline{\delta}}_{\mathrm{ML}}$ is needed for the unknown positions of the component solitons, the ML estimate $\hat{\underline{\delta}}_{\mathrm{ML}}$ can be simply formulated from $i_N(t)$ using matched filters. Since the ML estimates based on $r(t)$ and $i_N(t)$ must be the same, as shown in Section VI, then the detection performance of a generalized likelihood ratio test using those estimates and the signal $i_N(t)$ must also be the same.

At high SNR, the noise component of the signal $i_N(t)$ can be well modeled as bandlimited white Gaussian noise, as in Section VI. Therefore, the generalized likelihood ratio test for detection can be performed by first demultiplexing $r(t)$ with the Toda lattice equations followed by matched filter processing. We have therefore reduced generalized detection from a case where the composite signal $r(t)$ varies significantly as a function of the unknown parameters to one in which each of the separated component solitons varies through only a time shift. This reduces the complexity significantly while maintaining Bayes optimality.

To illustrate this detection algorithm, a hypothesis test between H_0 and H_{12} is considered, where the separation of the two solitons $\delta_1 - \delta_2$ is varied randomly in the interval $[-1/\beta_2,\, 1/\beta_2]$. A set of Monte Carlo runs has been completed

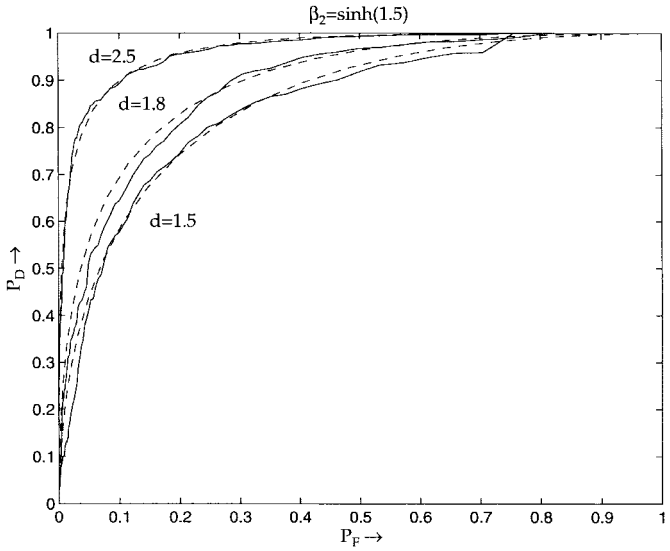

Fig. 14. Set of empirically generated receiver operating characteristics are shown for the detection of the smaller soliton from a two-soliton signal. For each of the three noise levels, the receiver operating characteristic for detection of the smaller soliton alone is also indicated with the dashed line, along with the corresponding detection index d.

for each of three different levels of the noise power N_0. The receiver operating characteristic for the soliton with $\beta_2 = \sinh(1.5)$ is shown in Fig. 14, where the probability of detection P_D for this soliton is shown as a function of the false alarm probability P_F. For comparison, the receiver operating characteristic that would result from a detection of the soliton alone at the same noise level and with the time-of-arrival known is also shown. The detection index $d = \sqrt{E/N_0}$ is indicated for each case, where E is the energy in the component soliton. The corresponding results for the larger soliton are qualitatively similar, although the detection indices for that soliton alone, with $\beta_1 = \sinh(2)$, are 5.6, 4.0, and 3.3, respectively. Therefore, the detection probabilities are considerably higher for a fixed probability of false alarm. Note that the detection performance for the smaller soliton is well modeled by the theoretical performance for detection of the smaller soliton alone. This implies, at least empirically, that the ability to detect the component solitons in a multiplexed soliton signal is unaffected by multiplexing with other solitons. Further, although the unknown relative separation results in significant waveform uncertainty and would require a prohibitively complex receiver for standard detection techniques, Bayes optimal performance can still be achieved with a minimal increase in complexity.

VIII. Concluding Comment

This paper can be viewed as an exploration of some of the properties of soliton signals and systems from the framework

$$\frac{dv(t)}{d\delta_2} = \frac{(2\beta_1^2\,\mathrm{sech}^2(\beta_1 t) + 2\beta_2^2\,\mathrm{sech}^2(\eta_2) + 2A\,\mathrm{sech}^2(\beta_1 t)\,\mathrm{sech}^2(\eta_2))}{\left(\cosh\left(\frac{\phi}{2}\right) + \sinh\left(\frac{\phi}{2}\right)\,\tanh(\beta_1 t)\,\tanh(\eta_2)\right)^3} \times \sinh\left(\frac{\phi}{2}\right)\,\tanh(\beta_1 t)(1-\tanh^2(\eta_2))\beta_2 + \frac{2\beta_2^3\,\mathrm{sech}^2(\eta_2)\,\tanh(\eta_2) + 2A\,\mathrm{sech}^2(\beta_1 t)\,\mathrm{sech}^2(\eta_2)\,\tanh(\eta_2)\beta_2}{\left(\cosh\left(\frac{\phi}{2}\right) + \sinh\left(\frac{\phi}{2}\right)\,\tanh(\beta_1 t)\,\tanh(\eta_2)\right)^2} \tag{30}$$

$$\begin{aligned}\left.\frac{d^2v(t)}{d\delta_2^2}\right|_{\delta_2=0} =& \frac{4\beta_2^4\mathrm{sech}(\tau_2)^2\tanh(\tau_2)^2 - 2\beta_2^4\mathrm{sech}(\tau_2)^2(1-\tanh(\tau_2)^2)}{\left(\cosh\left(\frac{\phi}{2}\right) + \sinh\left(\frac{\phi}{2}\right)\tanh(\tau_1)\tanh(\tau_2)\right)^2} \\ &+ \frac{4A\mathrm{sech}(\tau_1)^2\mathrm{sech}(\tau_2)^2\tanh(\tau_2)^2\beta_2^2 - 2A\mathrm{sech}(\tau_1)^2\mathrm{sech}(\tau_2)^2(1-\tanh(\tau_2)^2)\beta_2^2}{\left(\cosh\left(\frac{\phi}{2}\right) + \sinh\left(\frac{\phi}{2}\right)\,\tanh(\tau_1)\tanh(\tau_2)\right)^2} \\ &+ \frac{(8\beta_2^3\mathrm{sech}(\tau_2)^2\tanh(\tau_2) + 8A\mathrm{sech}(\tau_1)^2\mathrm{sech}(\tau_2)^2\tanh(\tau_2)\beta_2)\sinh\left(\frac{\phi}{2}\right)\tanh(\tau_1)(1-\tanh(\tau_2)^2)\beta_2}{\left(\cosh\left(\frac{\phi}{2}\right) + \sinh\left(\frac{\phi}{2}\right)\tanh(\tau_1)\tanh(\tau_2)\right)^3} \\ &+ \frac{(6\beta_1^2\mathrm{sech}(\tau_1)^2 + 6\beta_2^2\mathrm{sech}(\tau_2)^2 + 6A\,\mathrm{sech}(\tau_1)^2\mathrm{sech}(\tau_2)^2)\sinh\left(\frac{\phi}{2}\right)^2\tanh(\tau_1)^2(1-\tanh(\tau_2)^2)^2\beta_2^2}{\left(\cosh\left(\frac{\phi}{2}\right) + \sinh\left(\frac{\phi}{2}\right)\,\tanh(\tau_1)\tanh(\tau_2)\right)^4} \\ &+ \frac{(4\beta_1^2\mathrm{sech}(\tau_1)^2 + 4\beta_2^2\mathrm{sech}(\tau_2)^2 + 4A\,\mathrm{sech}(\tau_1)^2\mathrm{sech}(\tau_2)^2)\sinh\left(\frac{\phi}{2}\right)\tanh(\tau_1)\tanh(\tau_2)(1-\tanh(\tau_2)^2)\beta_2^2)}{\left(\cosh\left(\frac{\phi}{2}\right) + \sinh\left(\frac{\phi}{2}\right)\tanh(\tau_1)\tanh(\tau_2)\right)^3}\end{aligned} \tag{33}$$

of a communication paradigm. Many of the issues that arise in the analysis of this potential communication system are derived from detection and parameter estimation of the transmitted multisoliton signals, including soliton multiplexing, energy compaction, and enhanced estimation and detection performance. Although the multiplexed communication techniques suggested in this paper are highly simplified, they serve to illustrate that with their rich properties, tractability, and relatively simple hardware implementations, soliton signals and systems more generally may ultimately form the basis of advanced systems for a wide variety of communication and signal processing applications. Possible applications include power-efficient joint modulators and multiplexors. These systems could operate purely in analog and be nonlinear, yet have performance that is characterized in closed form.

APPENDIX

A. Proof of Energy Minimization for Two-Soliton Solution

Without loss of generality, we assume $\delta_1 = 0$ and seek the value of δ_2 that minimizes (11). Differentiation of (11) yields

$$\frac{dE}{d\delta_2} = \int_{-\infty}^{\infty} 2v(t)\,\frac{dv(t)}{d\delta_2}\,dt. \tag{29}$$

We now seek the value of δ_2 that makes the integral (29) equal to zero. This is accomplished by first noting that when $\delta_1 = \delta_2$ in (10), then $v(t)$ is an even function of time, centered about $\delta_1 = \delta_2$. In this case, setting $\delta_2 = \delta_1 = 0$ makes $v(t)$ even. If it can be shown that by setting $\delta_2 = 0$ that $dv(t)/d\delta_2$ is an odd function, then the integral in (29) is trivially zero. This indeed turns out to be the case in (30), shown at the bottom of the previous page. Note that setting $\delta_2 = 0$ makes each of the terms in the numerator of the first term of (30) even. Setting $\delta_2 = 0$ also makes the denominator of the first term an even function. This term is then multiplied by the second term of (30), which is a constant $\sinh(\phi/2)$ times an odd function $\tanh(\beta_1 t)$ times an even function. Hence, we have several even functions multiplying an odd function, making the entire first line in (30) an odd function. The second line is also seen to be an odd function by similar analysis. As a result, $\delta_2 = 0$ is a stationary point of (11). To check that this is a minimum, we need to verify that

$$\frac{d^2}{d\delta_2^2}\int_{-\infty}^{\infty} v^2(t)\,dt\bigg|_{\delta_2=0} > 0. \tag{31}$$

First, we note that

$$\frac{d^2}{d\delta_2^2}\int_{-\infty}^{\infty} v^2(t)\,dt\bigg|_{\delta_2=0} = \int_{-\infty}^{\infty} 2\left(\frac{dv(t)}{d\delta_2}\bigg|_{\delta_2=0}\right)^2 + 2v(t)\,\frac{d^2v(t)}{d\delta_2^2}\bigg|_{\delta_2=0} dt. \tag{32}$$

Since $dv(t)/d\delta_2|_{\delta_2=0}$ is real, the first term in (32) is positive. The second term contains $v(t)$, which is real and positive, and $d^2v(t)/d\delta_2^2|_{\delta_2=0}$, which can be seen to also be positive, as in (33), shown at the bottom of the previous page, where $\tau_i = \beta_i t$. Since each term in (32) is positive, the integral is therefore positive, and $\delta_2 = \delta_1$ is indeed a minimum.

ACKNOWLEDGMENT

We thank the associate editor Prof. A. Sayed and the anonymous reviewers for their detailed comments that considerably improved the clarity of the paper.

REFERENCES

[1] M. Ablowitz and A. Clarkson, *Solitons, Nonlinear Evolution Equations and Inverse Scattering.* Cambridge, U.K.: Cambridge Univ. Press, 1991.
[2] E. Infeld and G. Rowlands, *Nonlinear Waves, Solitons and Chaos.* New York: Cambridge Univ. Press, 1990.
[3] A. Scott, F. Chu, and D. McLaughlin, "The soliton: A new concept in applied science," *Proc. IEEE,* vol. 61, pp. 1443–1483, Oct. 1973.
[4] M. Toda, "Nonlinear lattice and soliton theory," *IEEE Trans. Circuits Syst.,* vol. CAS-30, pp. 542–554, Aug. 1983.
[5] A. Scott, *Active and Nonlinear Wave Propagation in Electronics.* New York: Wiley-Interscience, 1970.
[6] R. Hirota and K. Suzuki, "Theoretical and experimental studies of lattice solitons in nonlinear lumped networks," *Proc. IEEE,* vol. 61, pp. 1483–1491, Oct. 1973.
[7] A. Singer, "A new circuit for communication using solitons," in *Proc. IEEE Workshop Nonlinear Signal Image Process.,* 1995, vol. I, pp. 150–153.
[8] M. Rodwell *et al.,* "Active and nonlinear wave propagation devices in ultrafast electronics and optoelectronics," *Proc. IEEE,* vol. 82, pp. 1035–1059, July 1994.
[9] H. A. Haus, "Molding light into solitons," *IEEE Spectrum,* pp. 48–53, Mar. 1993.
[10] Y. Cho, J. Wakita, and N. Miyagawa, "Nonlinear equivalent circuit model analysis of acoustic devices and propagation of surface acoustic wave," *Jpn. J. Appl. Phys.,* vol. 32, no. 5B, pp. 2261–2264, 1993.
[11] A. Osborne, E. Segre, G. Boffetta, and L. Cavaleri, "Soliton basis states in shallow-water ocean surface waves," *Phys. Rev. Lett.,* vol. 67, pp. 592–595, July 1991.
[12] R. Jenkins, J. Sauer, C. Radehaus, A. Benner, M. Ablowitz, and G. Beylkin, "Techniques for detecting densely wavelength-multiplexed solitons," in *Proc. SPIE—ISOE,* July 1993, vol. 2024, pp. 258–269.
[13] A. Singer, "Signal processing and communication with solitons," Ph.D. dissertation, Mass. Inst. Technol., Cambridge, 1996.
[14] A. Singer and A. Oppenheim, "Circuit implementations of soliton systems," *Int. J. Bifurc. Chaos,* vol. 9, no. 4, pp. 571–590, 1999.
[15] M. D. Trott, "Unequal error protection codes: Theory and practice," in *Proc. IEEE Inform. Theory Workshop,* June 1996, p. 11.
[16] M. Toda, *Theory of Nonlinear Lattices,* no. 20 in Springer Series in Solid-State Science. New York: Springer-Verlag, 1981, no. 20.
[17] N. Zabusky and M. Kruskal, "Interaction of solitons in a collisionless plasma and the recurrence of initial states," *Phys. Rev. Lett.,* vol. 15, pp. 240–243, Aug. 1965.
[18] K. Suzuki, R. Hirota, and K. Yoshikawa, "Amplitude modulated soliton trains and coding-decoding applications," *Int. J. Electron.,* vol. 34, no. 6, pp. 777–784, 1973.
[19] K. Suzuki, R. Hirota, and K. Yoshikawa, "The properties of phase modulated soliton trains," *Jpn. J. Appl. Phys.,* vol. 12, pp. 361–365, Mar. 1973.
[20] J. vomScheidt and W. Purkert, "Random eigenvalue problems," *Probability and Applied Mathematics.* Amsterdam, The Netherlands: North Holland, 1983.
[21] H. L. V. Trees, *Detection, Estimation, and Modulation Theory: Part I.* New York: Wiley, 1968.

Andrew C. Singer (M'96), for a photograph and biography, see this issue, p. 2699.

Alan V. Oppenheim (F'77) received the S.B. and S.M. degrees in 1961 and the Sc.D. degree in 1964, all in electrical engineering, from the Massachusetts Institute of Technology (MIT), Cambridge. He was also the recipient of an honorary doctorate from Tel-Aviv University, Tel-Aviv, Israel, in 1995.

In 1964, he joined the faculty at MIT, where he currently is the Ford Professor of Engineering and a MacVicar Faculty Fellow. Since 1967, he has also been affiliated with MIT Lincoln Laboratory, Lexington, MA, and, since 1977, with the Woods Hole Oceanographic Institution, Woods Hole, MA. His research interests are in the general area of signal processing and its applications. He is coauthor of the widely used textbooks *Discrete-Time Signal Processing* and *Signals and Systems*. He is also editor of several advanced books on signal processing.

Dr. Oppenheim is a Member of the National Academy of Engineering and of Sigma Xi and Eta Kappa Nu. He has been a Guggenheim Fellow and a Sackler Fellow at Tel-Aviv University. He has also received a number of awards for outstanding research and teaching, including the IEEE Education Medal, the IEEE Centennial Award, the Society Award, the Technical Achievement Award, and the Senior Award of the IEEE Acoustics, Speech and Signal Processing Society. He has also received a number of awards at MIT for excellence in teaching, including the Bose Award and the Everett Moore Baker Award.

Gregory W. Wornell (M'91) received the B.A.Sc. degree (with honors) from the University of British Columbia, Victoria, B.C., Canada, and the S.M. and Ph.D. degrees from the Massachusetts Institute of Technology (MIT), Cambridge, all in electrical engineering, in 1985, 1987, and 1991, respectively.

Since 1991, he has been on the faculty of the Department of Electrical Engineering and Computer Science at MIT, where he is currently Cecil and Ida Green Career Development Associate Professor. From 1992 to 1993, he was on leave at AT&T Bell Laboratories, Murray Hill, NJ, and during 1990, he was a Visiting Investigator at the Woods Hole Oceanographic Institution, Woods Hole, MA. His current research interests include signal processing, wireless and broadband communications, and applications of fractal geometry and nonlinear dynamical system theory in these areas. He is author of the monograph *Signal Processing with Fractals: A Wavelet-Based Approach* and coeditor of the volume *Wireless Communications: Signal Processing Perspectives* (Englewood Cliffs, NJ: Prentice-Hall). He is also a consultant to industry and an inventor on four patents in the area of communications and another in the area of digital watermarking is pending.

Dr. Wornell is currently an Associate Editor for the communications area for IEEE SIGNAL PROCESSING LETTERS and serves on the Communications Technical Committee of the Signal Processing Society. Among the awards he has received for teaching and research are the MIT Goodwin Medal for "conspicuously effective teaching" in 1991, the ITT Career Development Chair at MIT in 1993, an NSF Faculty Early Career Development Award in 1995, an ONR Young Investigator Award in 1996, the MIT Junior Bose Award for Excellence in Teaching in 1996, and an MIT Graduate Student Council Teaching Award in 1998. He is a member of Tau Beta Pi and Sigma Xi.